Charge localization on a polymer surface measured by triboelectrically induced x-ray emission

Adam L. Collins,[1,*] Carlos G. Camara,[1,2] Brian B. Naranjo,[1] Seth J. Putterman,[1] and Jonathan R. Hird[1]
[1]*Department of Physics and Astronomy, University of California, Los Angeles, Los Angeles, California 90095, USA*
[2]*Tribogenics, 4040 Del Rey Avenue, Suite 1, Marina Del Rey, California 90292, USA*
(Received 2 February 2013; published 16 August 2013)

The means by which charge is exchanged between two surfaces that have been brought into contact is perhaps the longest standing unsolved problem in physics. To this day, it is debated as to whether charging is due to electrons or ions. Contact electrification is such a singular process that it lies beyond the scope of density functional theory and other *ab initio* theories of material structure. We present a new method for studying the fundamental processes that underlie triboelectrification, based upon the structure of x-ray emission from the interface of separating surfaces. Our measurement of the x-ray spectrum emitted from lead rolling against various thicknesses of unplasticized polyvinyl chloride (uPVC) on top of a grounded conductor indicate that triboelectrification, like turbulence, extends over a broad range of length scales. We observe millimeter-scale charge-patching, which indicates the feasibility of building MEMS x-ray sources.

DOI: 10.1103/PhysRevB.88.064202 PACS number(s): 41.20.Cv, 52.80.−s, 78.70.En, 84.37.+q

I. INTRODUCTION

Continuous media that are driven off-equilibrium display remarkable energy focusing effects. In sonoluminescence, a bubble concentrates the energy density of a standing sound wave by 12 orders of magnitude to create picosecond flashes of ultraviolet light.[1] When adhesive tape is peeled from a roll with a force of only 2 N, nanosecond x-ray pulses are emitted from the vertex with a flux that is sufficient to expose a photograph in seconds.[2] X-ray emission from surfaces in contact has its origins in triboelectrification: the ubiquitous phenomenon whereby charge is exchanged when two materials are brought into and out of contact. Triboelectrification is a process fundamental to lightning,[3] xerography,[4] barometer light,[5,6] and explosive powder ignition.[7] Although contact electrification has been studied for over two thousand years,[8] its explanation in terms of an *ab initio* theory is lacking to such an extent that it is still contested as to whether the primary charge entity is an ion[9] or an electron.[10] In this paper, we report a method that employs x-ray emission from triboelectrically charged surfaces to probe the unknowns of triboelectrification, finding that the charge is organized into macroscopic patches at millimeter-length scales.

Contact electrification can yield charge densities as high as 10^{13} e/cm^2, as reported by Harper[11] and Horn.[12] Under vacuum, where discharge is suppressed, pairs of triboelectrically charged surfaces have been shown to produce x-rays up to 40 keV in energy.[2,13–16] The emission of nanosecond x-ray pulses (with total pulse energy up to 10 GeV) has been interpreted as originating from charge densities of $\sigma \sim 10^{12}$ e/cm^2.[17] The electric field near such a charge density is $\sim 10^6$ V/cm. The 40-keV photon spectrum emitted from tribocharged surfaces implies an accelerating distance of about 400 μm. Can triboelectrification be used to reach higher photon energies by increasing the separation d between contacting materials that are subsequently separated? If charge is uniformly distributed on the surface, the potential V available to generate photons from a discharge of electrons would be

$$V \sim \frac{\sigma d}{\epsilon_0}. \quad (1)$$

Experiments with triboelectrically charged plates (such as in Refs. 16 and 18) found that at a fixed separation, the spectral density was unchanged as the flux decreased by an order of magnitude. One interpretation is that the materials do not acquire a uniform charge distribution. In fact, localization of triboelectric charge has been demonstrated at the submicron scale under atmospheric conditions.[19,20] Here, we use x-ray emission from contact electrification to probe the distribution of surface charge, revealing localization of charge even at millimeter-length scales.

II. EXPERIMENTAL

Figure 1 shows the vacuum apparatus used to explore correlations between x-ray emission and triboelectrification. Two aluminum rollers of 36.83-mm diameter were mounted in contact, with a force of 1 N. One roller was driven using a DC motor at a steady angular velocity of 5.87 rad/s, while the second roller was free to rotate about a parallel axis, driven by frictional contact with the first roller. To ensure good contact, the driven roller was tapered to a width of 3.18 mm at its periphery and coated in lead (Pb, cleaned with acetone and ethanol) bringing its diameter to 37.15 mm. The other roller was 12.7 mm wide, onto which integer layers of a 19-mm-wide pressure sensitive adhesive (PSA) tape (3M Scotch brand 600) were wound adhesive side down. The tape consists of an unplasticized polyvinyl chloride (uPVC) film with an acrylic-based adhesive. At pressures below ∼10 mTorr, the combination of lead and PSA tape provides a highly reliable, if rather unconventional, triboelectric x-ray generator. Pb acquires a large net-positive charge with respect to uPVC, which becomes net-negatively charged.[21] Bremsstrahlung radiation (x-rays) is generated as electrons are accelerated across the uPVC-Pb gap and into the lead.

The rolling apparatus and a solid state x-ray detector (Amptek XR-100T-CdTe) were placed in a vacuum chamber, evacuated to 5 mTorr. The detector input window (25 mm^2) was positioned perpendicular to and between 30 and 60 mm from the vertex of the contacting rollers. The detector was

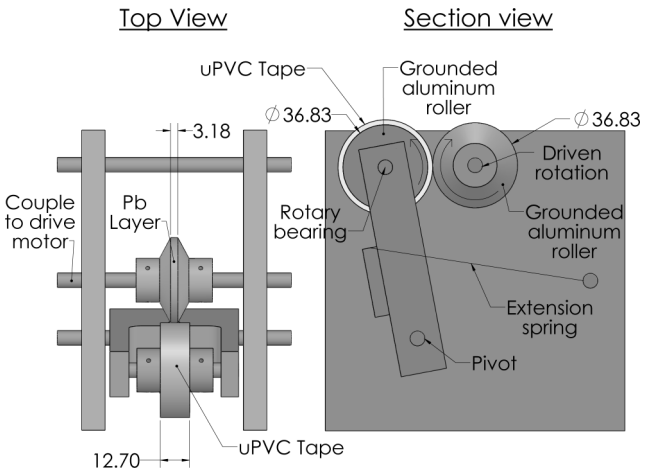

FIG. 1. Apparatus used to investigate nonuniform triboelectric charge distributions. All dimensions are in mm. A lead-coated roller is driven by a DC motor, while contacting a freely rotatable uPVC tape-coated roller. Under vacuum (< 10 mTorr), x-rays are generated from the interface of the two rollers.

placed further away for high-flux events, and closer for low-flux events. To avoid pile-up of x-ray photons (possible from nanosecond x-ray pulses[17]), a 0.56-mm-thick tungsten sheet, with a 0.69-mm-diameter pinhole, was placed in front of the 25-mm^2 detector; the detection area was reduced to 0.369 mm^2. Data were acquired by computer via a data acquisition board (National Instruments PXI-1033) at 1 MHz in six hundred 1-s windows. Data were processed using in-house software.

Roller systems are known to slowly acquire triboelectric charge before reaching a steady state.[22,23] Under vacuum conditions, the slow build-up of charge results in an initiation period during which the x-ray flux fluctuates violently (though the x-ray spectrum remains unchanged). Accordingly, the data

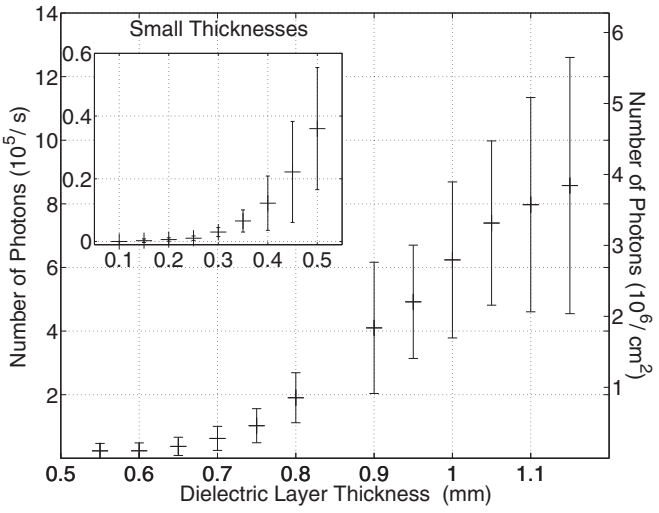

FIG. 2. Mean x-ray flux as a function of dielectric layer thickness, corrected for detector efficiency and solid angle sampled. Error bars represent the standard deviation about the mean. The inset shows the data for thin layers of tape, with the flux an order of magnitude lower. Left axis denotes flux by time; right axis denotes flux by contact area exposed.

reported here were taken 10 minutes after the rollers began rotating, when the emission had reached a steady state.

By changing the thickness of a dielectric layer via the number of winds of PSA tape (∼50 μm per layer), it was found that both the flux (Fig. 2) and energy (Fig. 3) of x-rays could be varied.

III. RESULTS

Figure 2 shows the mean number of x-ray photons recorded per second as a function of dielectric layer thickness; the error bars represent the standard deviation about the mean. There is a rapid increase in the production of x-rays when a thickness of about 0.7 mm is reached. As further layers of tape are applied, the x-ray flux continues to rise (rising the most rapidly at ∼0.95 mm) before plateauing from around 1.2 mm.

The spectral envelope was also observed to change as a function of dielectric layer thickness (Fig. 3), with thinner layers providing lower energy photons. With a thick enough dielectric layer (>∼0.5 mm), it is possible to stimulate the L_α and L_β lines of Pb. Figure 4 shows the high-energy cut-off of the x-ray spectra as a function of dielectric layer thickness, which is equated with the maximum field available to accelerate charge across the uPVC-Pb gap. The cut-off energy rises with dielectric layer thickness and saturates at ∼40 keV.

The experiment was repeated a number of times to confirm the result. While the magnitude of the flux was observed to change between repeats by up to a factor of five, the shape of the flux as a function of uPVC layer thickness remained unchanged. The same spectrum was consistently produced for a given thickness of uPVC.

An additional experiment was carried out in which the 12.7-mm-wide aluminum roller was replaced with an insulating one made of nylon 6,6 having identical dimensions. The experiment was repeated using the nylon roller and multiple layers of tape. In Fig. 5, it can be seen that x-rays

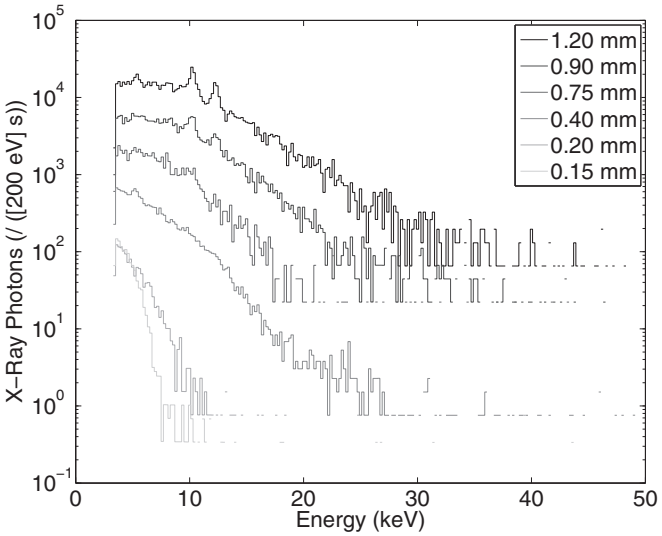

FIG. 3. Energy spectra of the photons emitted from different thicknesses of uPVC tape rolling against lead in a 5-mTorr vacuum. Data are corrected for detector efficiency and solid angle sampled.

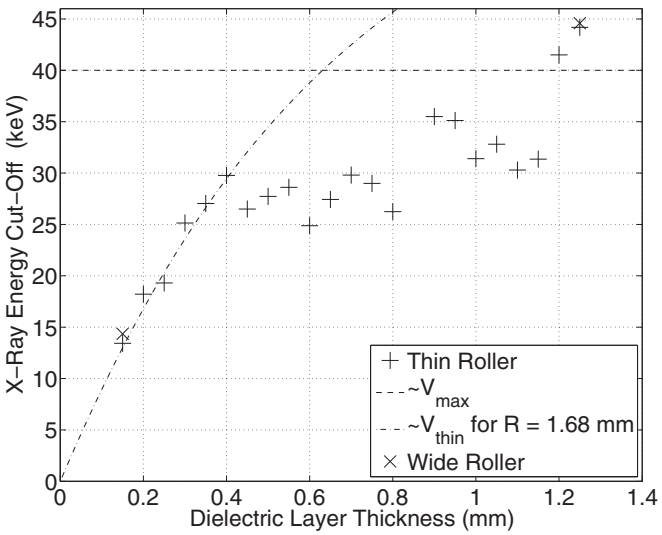

FIG. 4. High-energy cut-off of the x-ray spectrum as a function of dielectric layer thickness. At thicker layers ($> \sim 1$ mm), the energy cut-off saturates at ~40 keV. For thin layers ($< \sim 0.4$ mm), the cut-off energy reduces with thickness. V_{max} and V_{thin} from Eqs. (4) and (5) are also shown, fitted to the "Thin Roller" data. "Wide Roller" data are from an identical experiment but with the lead roller being four times wider.

emitted from the nylon roller system have flux and spectra that change little with PSA tape thickness. The extent to which the grounding plane screens the triboelectrically generated accelerating potential for thin layers of uPVC tape is apparent

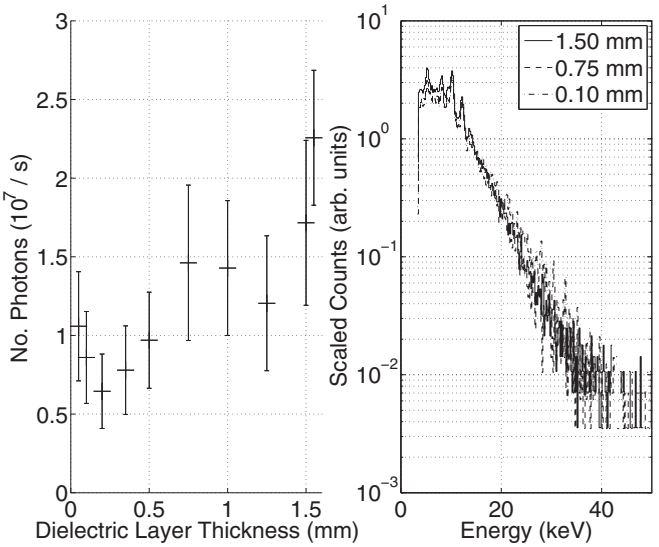

FIG. 5. Data for x-ray photons generated by Pb rolling against uPVC tape wound onto a nylon 6,6 roller of identical dimensions to those shown in Fig. 1. Left figure: Mean x-ray flux as a function of dielectric layer thickness. Error bars represent the standard deviation about the mean. The flux changes little with dielectric layer thickness. Right figure: Energy spectra for three different layer thicknesses. The recorded spectra have been scaled to similar magnitudes in order to show the equivalence of the spectral envelope at differing dielectric layer thicknesses.

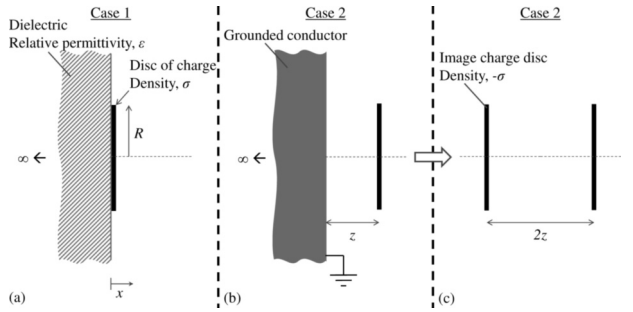

FIG. 6. Disk of charge in the presence of media, to model the triboelectric charge on the surface of uPVC tape. (a) Disk of charge on the surface of a dielectric material; this represents the thick film limit. (b) Disk of charge set off from the surface of a conductor by a distance z; this represents the thin film limit. (c) Electrostatic equivalent of (b), the conductor is replaced with an identically sized disk with opposite charge, a distance $2z$ from the original charge disk.

from a comparison of Figs. 2, 3, and 5. The screening of the field reduces both x-ray flux and energy.

IV. INTERPRETATION

We interpret the data of Figs. 3–5 as resulting from patches of localized charge on the surface of the uPVC tape. To obtain a scale for the size of a localized charge patch, an electrostatic model is applied to calculate how the position of a grounding plane (aluminum roller) affects the field generated by a disk of charge. The maximum potential at the surface of the disk can be equated with the peak x-ray energy measured.

For an isolated disk of charge, density σ, radius R, the potential at a distance x along a perpendicular axis is

$$V = -\frac{\sigma}{2\epsilon_0}(|x| - \sqrt{x^2 + R^2}); \tag{2}$$

hence, the potential at the surface of the disk is

$$V_0 \to \frac{\sigma R}{2\epsilon_0}. \tag{3}$$

The presence of media changes the potential at the surface of the disk; two cases were therefore considered, as illustrated in Fig. 6.

In the first case, for a thick layer of tape, we model the disk of charge on the surface of a semi-infinite dielectric, with relative permittivity ϵ [Fig. 6(a)]. The presence of the dielectric layer screens the charge, and reduces the potential at the surface of the disk to

$$V_{max} = \frac{2}{\epsilon + 1} V_0. \tag{4}$$

In the second case, for thin layers of tape, the dielectric layer is neglected, and the disk is set off from a grounded conducting plane by a distance z [Fig. 6(b)]. z is the thickness of the tape layer. The conducting plane is replaced with an image charge disk [Fig. 6(c)] that reduces the potential at the surface of the original disk to

$$V_{thin} = V_0\left(1 + \frac{2z}{R} - \sqrt{1 + \frac{4z^2}{R^2}}\right). \tag{5}$$

From Fig. 4, V_{max} ~40 kV. The relative permittivity of uPVC is 3;[24] hence, V_0 ~80 kV. Using data at $z = 0.15$ mm for the thin layer approximation, V_{thin} was measured to be ~13 kV, implying a disk radius of R ~1.68 mm. Considering V_0 again, with R = 1.68 mm, the charge density is $\sim 5 \times 10^{11}$ e/cm^2. Equations (4) and (5) are plotted in Fig. 4, with the given values of R and σ; the data are consistent with a triboelectrically induced charge localized to a ~1-mm region.

With the calculated disk diameter being so similar to the width of the Pb-coated roller, an additional experiment was performed to check whether the calculated disk size was geometry-imposed. The x-ray spectrum was measured for uPVC tape thicknesses of 0.15 and 1.25 mm rolling against a 12.7-mm-wide Pb-coated roller. As shown in Fig. 4, the x-ray cut-off energy was the same as that measured using the 3.18-mm-wide Pb-coated roller. The patch radius ($R \sim 1.68$ mm) is not due to the width of the Pb-coated roller.

The charge localization (R) and density (σ) are likely material properties of the uPVC tape, and are not affected by the external field because the forces at the molecular scale are much larger. Accordingly, under the current model, higher energy x-rays should be achievable with materials that provide a larger R or σ under contact electrification. Finding or engineering such materials is a clear goal for development of higher energy, triboelectrically driven MEMS-type x-ray devices.[18]

V. CONTEXT

Charge localization on the millimeter scale is four orders of magnitude larger than the scale of charge localization reported elsewhere.[19] We propose that in addition to charge localization at tens and hundreds of nanometers, as reported in Ref. 19, organization persists up to at least millimeter lengthscales. It is, however, the larger scale millimeter localization that is responsible for the electric fields large enough to accelerate charged particles to x-ray energies. Our data provide further evidence for the multiscale nature of triboelectrification; similar multiscale behavior has been reported for surface roughness, which could contribute to localization of charge.[25–28]

Charge densities to be expected from triboelectrification under atmospheric pressure are usually ~10^9–10^{10} e/cm^2,[11] while Ref. 19 reports localized charge densities of ~10^{13} e/cm^2. The net charge density reported here under vacuum lies within this range. When the local charge is averaged over a larger surface, the apparent density reduces. Conversely, if the millimeter-scale patches are composed of very high-density charge localized to sub-micron scales, a smaller net-charge density over the millimeter scale is expected.

VI. SUMMARY

Rolling lead against uPVC tape in a 5-mTorr vacuum provides a consistent source of triboelectrically generated x-rays. By changing the thickness of the uPVC layer on a grounded conductor, the x-ray flux and spectrum change, with thinner layers providing less flux and lower energy photons. For layers of uPVC greater than ~1 mm, the peak x-ray energy saturates at ~40 keV. It is concluded that the charge on the surface of the uPVC layer is localized to millimeter-scale regions of higher charge density than normally expected from triboelectrification. While there are reports of localization simultaneously at the nanoscale and microscale, we provide evidence for additional localization at the milliscale. Interactions over the milliscale are responsible for the discharge to x-rays. From a practical perspective, a charge density of $\sim 5 \times 10^{11}$ e/cm^2 over a 2-mm^2 area implies a potential V_0 of ~40 kV, allowing construction of MEMS-type devices to be possible with 40 kV pixel.

ACKNOWLEDGMENTS

This research was made possible by funding from USAMRMC/TATRC under Contracts No. W81XWH-10-1-1049 and No. W81XWH-12-1-0539.

*alcollins@physics.ucla.edu

[1] S. J. Putterman and K. R. Weninger, Annu. Rev. Fluid Mech. **32**, 445 (2000).
[2] C. Camara, J. Escobar, J. Hird, and S. Putterman, Nature (London) **455**, 1089 (2008).
[3] D. Petersen, M. Bailey, W. H. Beasley, and J. Hallett, J. Geophys. Res.: Atmospheres **113**, D17205 (2008).
[4] D. M. Pai and B. E. Springett, Rev. Mod. Phys. **65**, 163 (1993).
[5] J. Picard, Mem. Acad. Roy. Sci. (Paris) **10**, 566 (1676).
[6] R. Budakian, K. Weninger, R. Hiller, and S. Putterman, Nature (London) **391**, 266 (1998).
[7] F. Bowden and A. Yoffe, Res.: J. Sci. Appl. **1**, 581 (1948).
[8] P. O'Grady, *Thales of Miletus: The Beginnings of Western Science and Philosophy* (Ashgate, Farnham, UK, 2002).
[9] L. S. McCarty and G. M. Whitesides, Angew. Chem., Int. Ed. **47**, 2188 (2008).
[10] C. Liu and A. Bard, Nat. Mater. **7**, 505 (2008).
[11] W. Harper, *Contact and Frictional Electrification*, edited by Willis Jackson, H. Frölich, and N. F. Mott (Clarendon Press, London, 1967).
[12] R. G. Horn and D. T. Smith, Science **256**, 362 (1992).
[13] J. W. Obreimoff, Proc. R. Soc. London Series A **127**, 290 (1930).
[14] V. Karasev, N. Krotova, and B. Deryagin, Dokl. Akad. Nauk. SSR **88**, 777 (1953).
[15] V. Klyuev, Y. Toporov, A. Aliev, A. Chalykh, and A. Lipson, Sov. Phys. Tech. Phys **34**, 361 (1989).
[16] J. R. Hird, C. G. Camara, and S. J. Putterman, Appl. Phys. Lett. **98**, 133501 (2011).
[17] C. Camara, J. Escobar, J. Hird, and S. Putterman, Appl. Phys. B **99**, 613 (2010).
[18] S. Kneip, Nature (London) **473**, 455 (2011).
[19] H. T. Baytekin, A. Z. Patashinski, M. Branicki, B. Baytekin, S. Soh, and B. A. Grzybowski, Science **333**, 308 (2011).

[20]C. A. Rezende, R. F. Gouveia, M. A. da Silva, and F. Galembeck, J. Phys.: Condens. Matter **21**, 263002 (2009).
[21]A. Diaz and R. Felix-Navarro, J. Electrost. **62**, 277 (2004).
[22]R. G. Cunningham and T. J. Coburn, J. Appl. Phys. **37**, 2931 (1966).
[23]W. D. Greason, J. Electrost. **49**, 245 (2000).
[24]Kaye & Laby Online, Version 1.0 (2005), "Tables of physical & chemical constants" NPL, (1995), Chap. Dielectric properties of materials, p. 2.6.5, 16th ed.
[25]B. N. J. Persson, O. Albohr, U. Tartaglino, A. I. Volokitin, and E. Tosatti, J. Phys.: Condens. Matter **17**, R1 (2005).
[26]P. Lazić and B. N. J. Persson, Europhys. Lett. **91**, 46003 (2010).
[27]B. N. J. Persson, A. Kovalev, M. Wasem, E. Gnecco, and S. N. Gorb, Europhys. Lett. **92**, 46001 (2010).
[28]B. N. J. Persson, M. Scaraggi, and A. I. Volokitin, arXiv:1305.2709 [cond-mat.soft] (2013).